Modeling of Magnetic Flux Leakage Measurements of Steel Pipes

Till SCHMITTE, Salzgitter Mannesmann Forschung GmbH, Duisburg, Germany
Stefan NITSCHE, Andreas GROOS, Vallourec Mannesmann Tubes, Düsseldorf, Germany

Abstract. Using commercially available magnetic modeling software we have modeled the signal of Magnetic Flux Leakage (MFL) testing of steel pipes with different types of defects, including inside, outside and tilted notches in 2D. The results presented here show interesting dependencies of signal amplitude and width on the defect geometry, which may be useful for defect separation. The implemented method can easily be adopted for different testing geometries and pipe materials.

1. Introduction

One of the most important inspection techniques for seamless steel pipes is the magnetic stray flux (MFL) measurement. Any local variation of geometry or magnetic properties will change the stray field experienced by a sensor and will lead to an indication if some threshold is exceeded. Typically the threshold is calibrated by a reference measurement with a tube of the same geometry and material and a defined test-notch.

Although the stray field is directly correlated to the defect characteristics, type of defect separation still remains difficult and existing technologies are not always working satisfactory. For example the separation between inside and outside defects is usually done by analyzing the frequency content of the signal. A broader signal is assumed to be one of an inside defect, while sharper indications are assigned to outer defects. This technique has proved to work if the defects under investigation are test notches with the same width, however, may fail if one compares a small inside defect with a broad outside defect.

Obviously, a deeper understanding of the shape of the MFL signals is desirable in order to find more effective type-of-defect separation methods. Although some analytical approaches to calculate the MFL signal [1] [2] exist, the best solution for such kind of problems are numerical finite element methods. The first work concerning the calculation of MFL signals can be found in the work of Lord [3], followed by the work of Brudar [4], Förster [5] and Atherton [6]. In these early works only two dimensional problems with a comparably small amount of elements are discussed. Due to limited computer capabilities only some specific situations are modeled. More recent work is done by solving the MFL benchmark problems of the World Federation of Nondestructive Evaluation Centers [7]. Results to this include the work of Pignotti [8], Lunin [9], Zeng [10] and Ruch [11] . These studies are two and also three dimensional, however, very specific to the needs of the benchmark problem. There is also no discussion about the MFL signal of different defect types. Another recent study using three dimensional FEM analysis and yoke magnetization can be found in [12]. This study shows the MFL signal amplitude as a function of notch depth, width, length and lift-off, however, only a situation with yoke magnetization is modeled. No discussion of inside / outside defect-characteristic is given.

The MFL problem is generally a multi-parameter problem. The parameters can be grouped into setup dependent (yoke, magnetization current, gap …), pipe dependent (wall thickness, diameter, and material) and type of the defect dependent (inside / outside, width, length, depth, shape …). The above mentioned works only cover small sections of the complete parameter space, and several questions remain unanswered.

In this situation this work aims at filling some of the above mentioned gaps, a special focus lies on the separation of inside / outside defects. Therefore, one aim of this work is to verify some of the assumptions made by Orth [13] concerning a new technology of inside / outside defect separation.

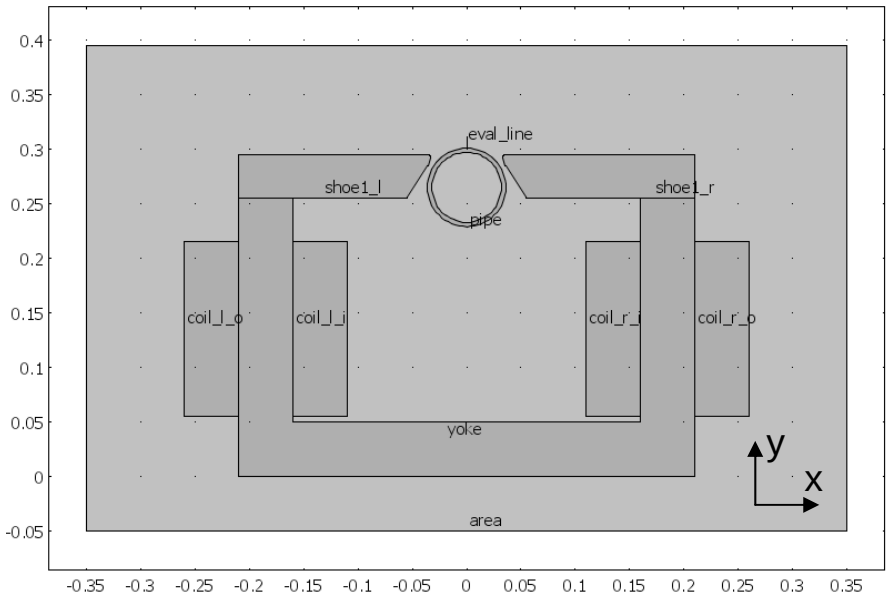

Figure 1: sketch of the setup used for the simulations. All measures are in meters.

2. Procedure

As mentioned above the complete MFL problem is a multi-dimensional one, even if we try to find some of the implicit systematic, reductions of the problem are necessary. First, only the 2D problem is discussed here. Practically this leads to qualitative information about the MFL signal shapes, the signal amplitude is too high in the FEM models compared to real measurements. The geometry modeled is a rotating pipe magnetized with an electromagnet. The problem is solved statically, i.e. the pipe is rotated step-wise and for each rotation angle the FEM problem is solved separately. The magnetic stray field is extracted from the solutions along a line perpendicular to the pipe surface, exactly between the pole shoes, i.e. the sensor is thought to be point-like, which could be a Hall-element or a GMR sensor [13]. Induction coils do not have a point-like behavior and deliver the field derivative; therefore they are not discussed here. From the remaining parameters further reductions are necessary. The complete set of parameters include

- Tube: WT, diameter, magnetization curve: material parameters
- Setup: gap, geometry of magnetizing circuit, magnetic field strength
- Rectangular notch: inside/outside, depth, width, tilt-angle
- Different shape of defects
- Lift-off, sensor-type

In this work we now report on we restrict ourselves to one specific geometry of the magnetizing circuit and one specific pipe (72x4 mm), but varying notch-parameters and lift-off. The magnetization curve of the pipe is chosen as in [7] and [9].

The computer simulations were performed using the general FEM-based software COMSOL [15] (in magnetostatic mode) together with MATLAB [16] as a scripting environment, leading to a complete parameterization of the problem. This allows us to recalculate all of the following results for different geometries of pipe or setup. Extensions of the presented work can be performed with only small modifications.

The geometry is taken from a laboratory setup as shown in **Figure 1**. Measurements of the magnetic induction B in the gap, inside the tube and at the sensor position confirm chosen model parameters. Usually symmetries can be used to reduce the amount of degrees of freedom of the FEM problem. In this work no symmetry exists parallel to the x-axis due to the special form of the magnetizing circuit and no symmetry parallel to the y-axis exists, because asymmetric defects, like tilted notches, break this symmetry. Clearly this leads to longer computation times but also to more general problem-formulation which might be helpful for future work. The actual FEM calculations are done in the following double-loop structure, which result in B_x and B_y as function of rotation angle and one geometry parameter:

A) calculate geometry (yoke, pipe, defect etc.) from given parameters and assign material parameters.
B) start with pipe-rotation at -10°:
   1. rotate pipe to new position
   2. automatically generate mesh
   3. solve using non-linear solvers
   4. extract B-field from solution for different lift-off values
   5. change rotation angle of pipe
   6. go back to 1 until pipe rotation is at +10°
C) change geometry parameter (e.g. notch-depth)
D) go back to A)

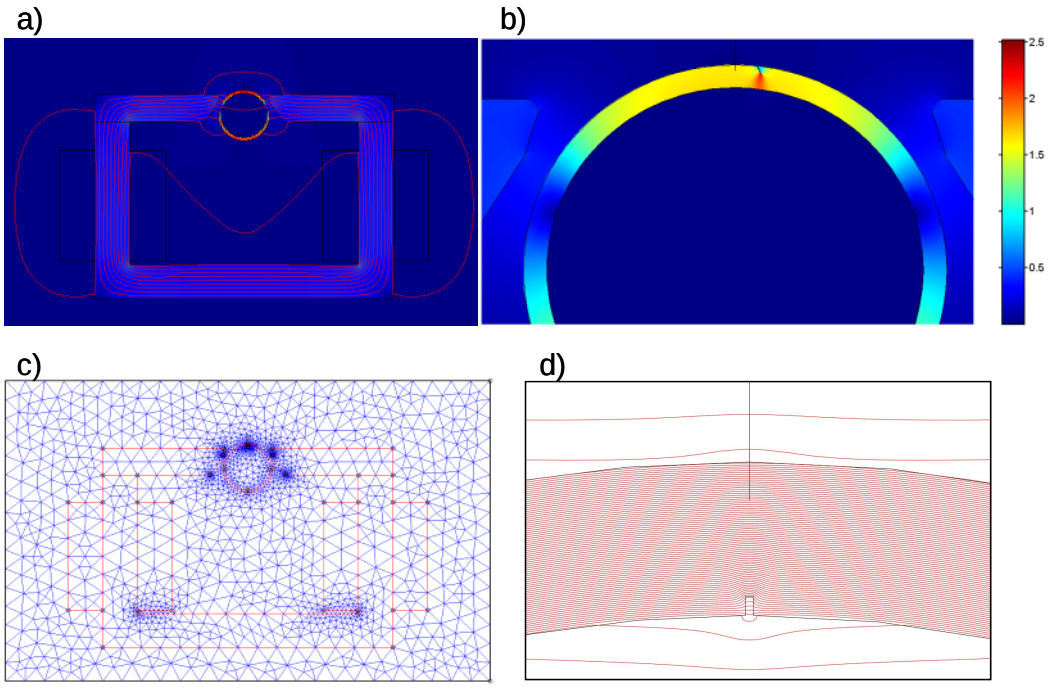

Figure 2: examples of simulation results: a) complete setup with flux lines. b) detail of a) showing an oblique outside notch at 10° position, the color-code gives the normalized B-field. c) view of the automatically generated mesh. Subfigure d) is a detailed view of flux lines around an inside notch.

In **Figure** 2 some examples of the calculations are shown. In a) a complete view of the modeled area is shown. The red lines are flux lines and the colours represent different strength of the magnetic induction $|B|$. In b) a close up of the area of pole-pieces, pipe and defect are displayed. The colors again represent $|B|$. As example an outside tilted notch is shown at a rotation angle position of approx. 10°. In **Figure** 2 d) a detailed view of an inside notch at 0° rotation angle is depicted. The red lines represent flux lines. It is obvious that the inside notch is a perturbation for the inside, defect near, flux lines but also the outside field is affected.

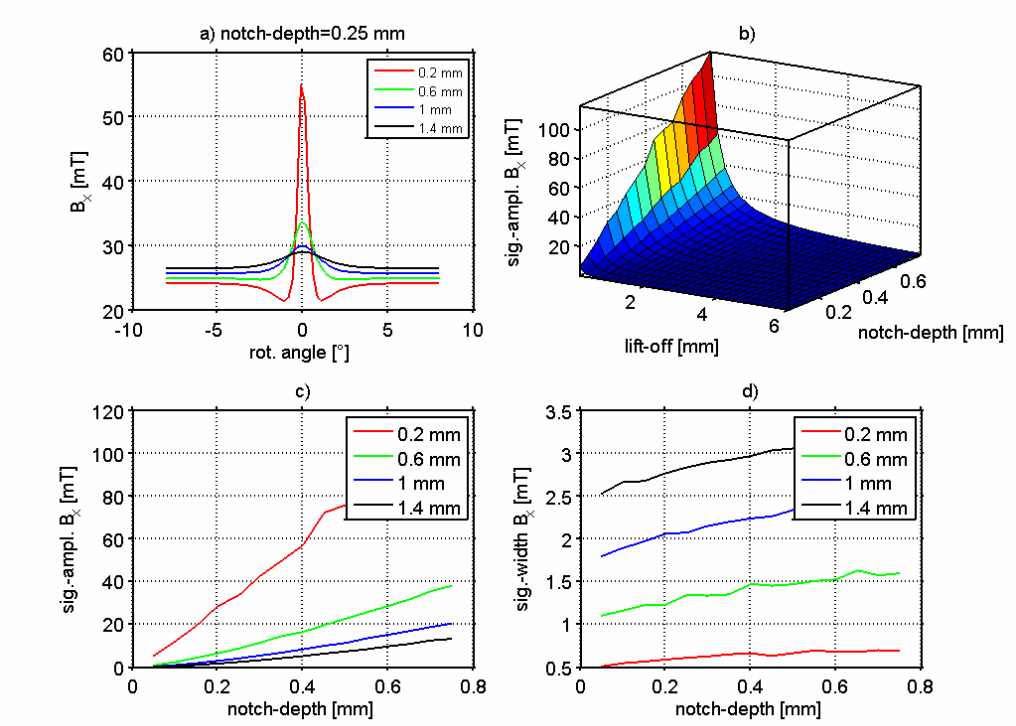

Figure 3: varying notch depth and lift-off of an outside notch: all above figures are results from a 72x4mm pipe, an outside notch with 0.2 mm width and a magnetizing current of 2 A. Subfigure a) shows some example results for a constant notch-depth of 0.25 mm but varying lift-off, as indicated in the figures legend. In b) the dependency of the signal amplitude as a function of notch depth and lift-off is displayed. Subfigures c) and d) show amplitude and width (FWHM) of the MFL signal, respectively, as a function of the notch depth for different lift-off values.

2. Results

During the simulation the magnetic induction with vector components B_x and B_y are calculated as a function of rotation angle, lift-off and notch-parameters. From this information the signal amplitude, the signal width and the signal asymmetry can be calculated. The signal amplitude is defined as max(B_x)-min(B_x). The signal width is defined to be the full width at half maximum (FWHM) of the signal peak. In the case of the oblique (tilted) notches it is useful to define signal asymmetry, which here is simply the difference between the two minima left and right from the main signal peak.

2.1 Outside Notch

We first discuss the MFL signal of an outside rectangular notch. In the first case the notch width is held constant while the notch depth is varied. Some of the results are shown in

Figure 3 where some example signals are plotted in subfigure a). As a second parameter we always have the lift-off, i.e. the distance between sensor and pipe surface. This parameter is of high practical relevance, as real installations always must find a good trade-off between having a good wear-protection and a small lift-off. In **Figure 3** a) the MFL signals for different lift-off values are given as indicated in the legend to that figure. It is apparent that the amplitude drastically decreases with increasing sensor distance, but also the signal shape changes, i.e. the pronounced minima next to the main peak are only found for very close inspection. The signal amplitude as a function of both lift-off and notch depth is shown in b). Here we see that the functionality of the lift-off dependence is exponential. The signal amplitude and signal width as function of notch-depth are displayed in c) and d). In the examined range the signal amplitude is almost a linear function of the notch depth, where the signal width only gradually increases with increasing defect depth.

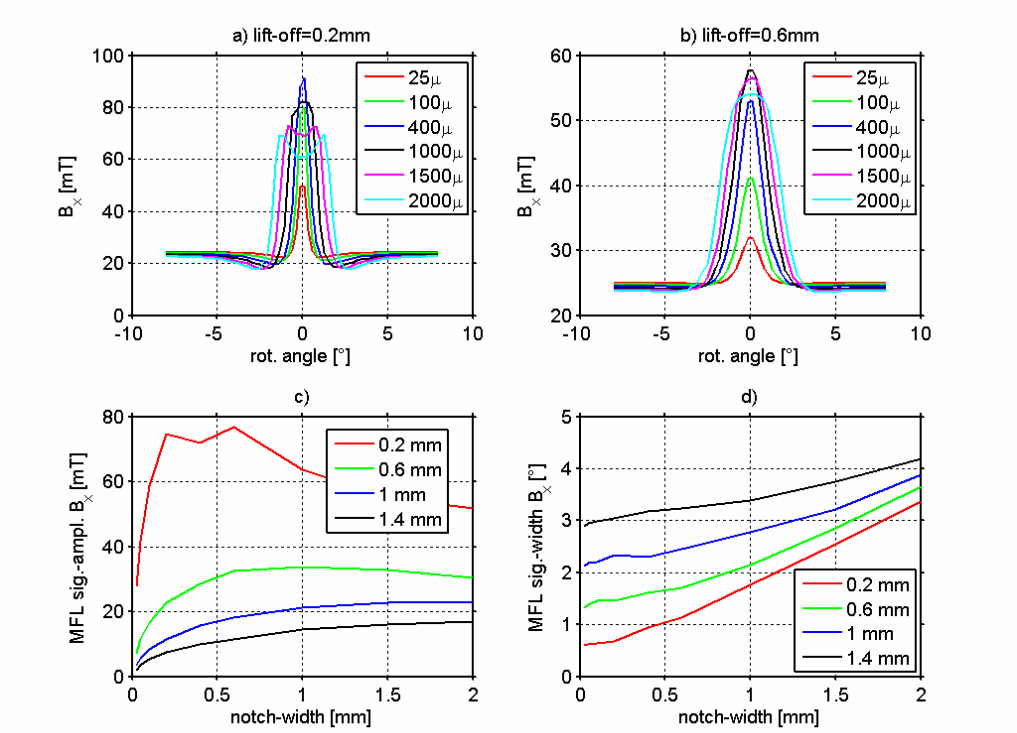

Figure 4: varying notch width and lift-off of an outside notch: above figures are results from a 72x4mm pipe, an outside notch with 0.5 mm depth and a magnetizing current of 2 A. Subfigures a) and b) display several simulated MFL signals for lift-off 0.2 mm and 0.6 mm, respectively, and for different notch-widths as given in the legend of the figures. In subfigure c) the signal amplitude (maximum – minimum) as a function of notch-width is plotted for different values of lift-off (see legend). In d) the signal-width (FWHM) is shown as in c).

Next, we examine the effect of changing the notch width and leaving the notch depth constant at 12.5%. The results are presented in **Figure 4**. In 4a) and b) some signals are plotted for constant lift-off of 0.2 mm and 0.6 mm, respectively. For the case of close inspection distance and broad notches (above 1mm) the single peak splits up into a double structure. In this situation the defect can be understood as a superposition of two step discontinuities. This also implies that the lateral resolution of the MFL technique is best with small lift-off, because it is clearly seen that for a larger lift-off value in b) the two steps can not be resolved.

The signal amplitude plotted in c) shows especially for small lift-off distances a pronounced maximum as a function of notch width. If the notch gets too small the amplitude decreases. If the notch gets broader and two steps get separated more and more

the signal amplitude is reduced and will reach a constant value which is the amplitude of one single step-like defect. As expected from this discussion the signal width plotted in d) is almost linear with notch-width.

In order to differentiate between several types of defects it may be interesting to be able to separate notch-like defects like cracks from oblique defects like slivers. Therefore we have modeled the MFL signal from a rectangular notch with comparably small width (0.1 mm). The notch is tilted, such that the depth measured along the notch direction is constant.

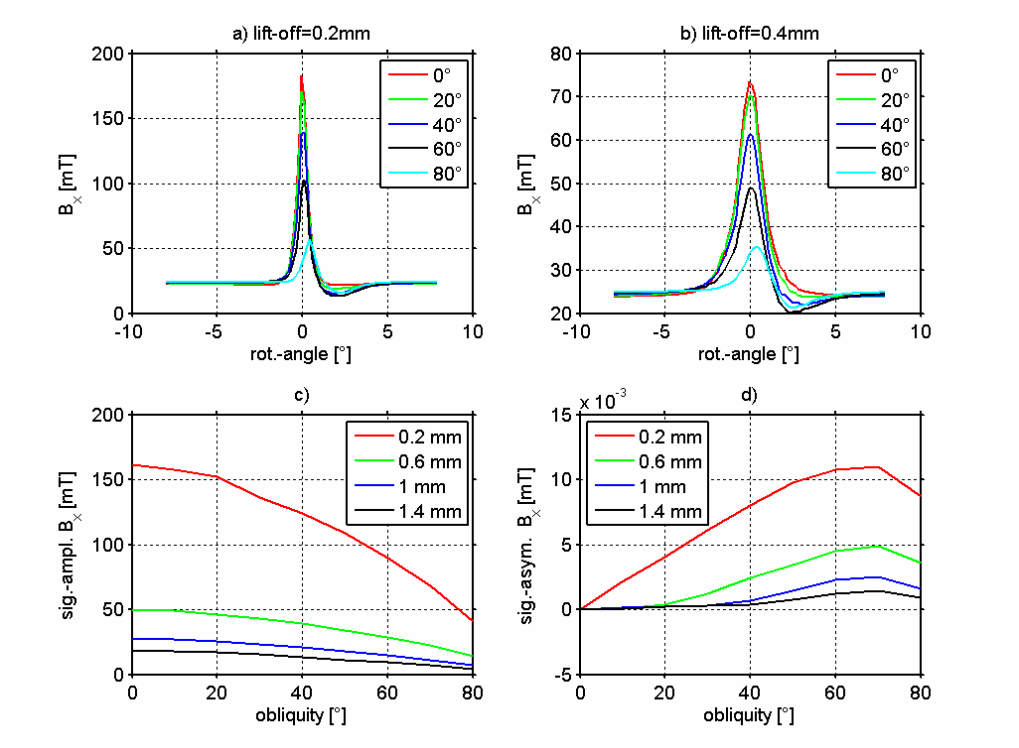

Figure 5: varying the obliquity of an outside notch: above figures are results from a 72x4mm pipe, an outside notch with 0.1 x 1.5 mm (width x depth) and a magnetizing current of 2 A. In subfigures a) and b) the MFL signals are displayed for two values of lift-off (0.2 and 0.4 mm) and a set of differently tilted notches, with obliquity angles as given in the legends of the figures. In d) the MFL signal amplitude as a function of the tilt angle of the notch is plotted for different lift-off values. Subfigure d) presents the calculated "asymmetry" (left minimum – right minimum) as a function of the tilt angle for different lift-off values.

In **Figure 5** some results of this calculation are presented. In 5a) and b) the lift-off is constant at 0.2 and 0.6 mm, respectively, and the obliquity is changing from 0° (no tilt angle) to 80° (nearly along the surface). There exists an asymmetry of the MFL signal which increases with tilt angle. This effect is stronger for small values of lift-off, the argument that the lateral resolution is best if the sensor is close to the surface holds as discussed before. In c) and d) the signal amplitude and asymmetry are plotted as a function of obliquity. It is seen that the amplitude always decreases if the notch is tilted. Interestingly, the asymmetry exhibits a maximum around 70° tilt angle. Not shown is the signal width as a function of tilt angle, which shows no dependency, i.e. remains constant.

2.2 Inside Notch

In this section the MFL signals of inside notches are discussed and compared to outside notches. Only examples are presented here. **Figure 6** displays the result of a calculation of varying notch depth of an inside rectangular notch. In a) and b) examples of MFL signals are recorded for a) constant lift-off and changing notch depth and b) constant notch and

changing lift-off. The results are summarized in c) and d) where the signal amplitude and signal width is plotted as a function of inside notch depth. In comparison to the outside notch we observe that the signal amplitude increases stronger than linear with notch depth and that the signal width slightly decreases as opposed to the outside case.

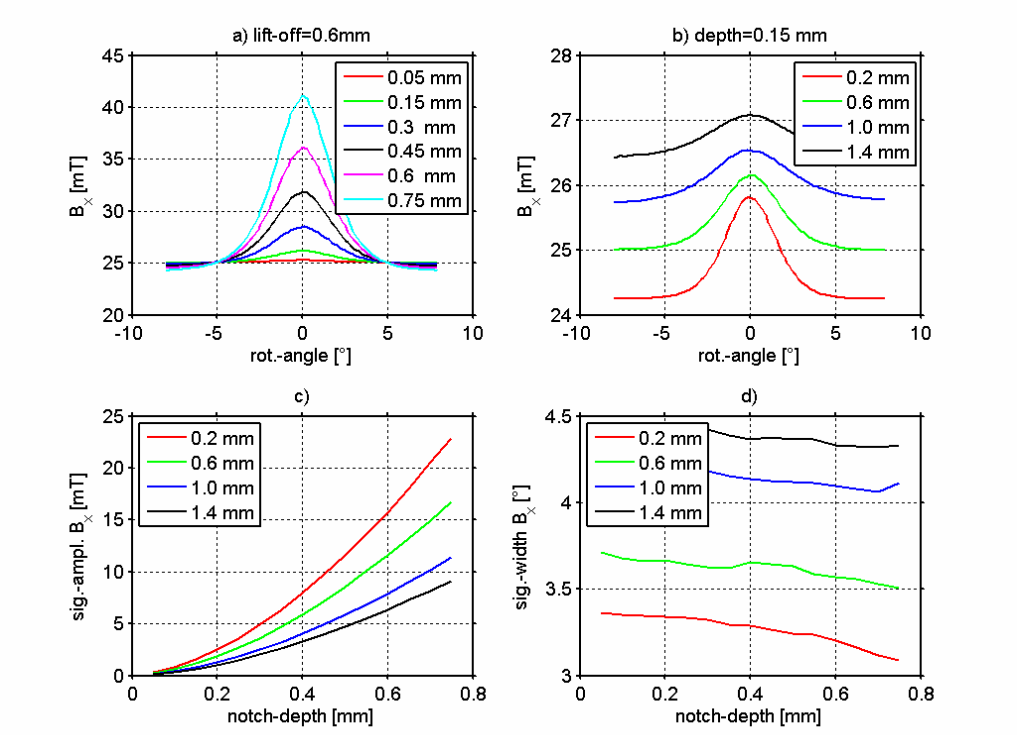

Figure 6: varying notch depth and lift-off of an inside notch: all above figures are results from a 72x4mm pipe, an inside notch with 0.2 mm width and a magnetizing current of 2 A. Subfigure a) displays simulated MFL signals at constant lift-off = 0.6 mm and different notch-depth. In b) the notch-depth is held constant at 0.15 mm and the signals for several values of the lift-off are presented. Subfigures c) and d) show the MFL signal amplitude and signal width (FWHM), respectively, as a function of the notch-depth for different values of lift-off.

2.3 Comparison of Inside / Outside Defects

In **Figure 7** a) and b) a direct comparison of MFL signals modeled for the case of outside and inside notch is given. As expected the signal width is much larger for the inside notch and the signal amplitude is larger for the outside notch. Comparing the signal width for the smallest inside notch and a broader outside notch one can clearly see that there are problems in inside / outside separation if one takes the signal width into account only. The solution to this problem as reported in [13] solves this ambiguity by measuring the MFL signal with Hall or GMR sensors in different lift-off distances. Experimentally they found a different decay rate of the signal with increasing surface distance for inside and outside defects. This work does verify these measurements as is shown in **Figure 7** c) by plotting the calculated signal amplitude of inside and outside signal as a function of lift-off. Moreover, in [13] it is stated that the relation between the signals obtained from two sensors at different lift-off is approx. 0.3 for inside defects and 0.15 for an outside defect. This is also perfectly reproduced by our calculation as shown in d).

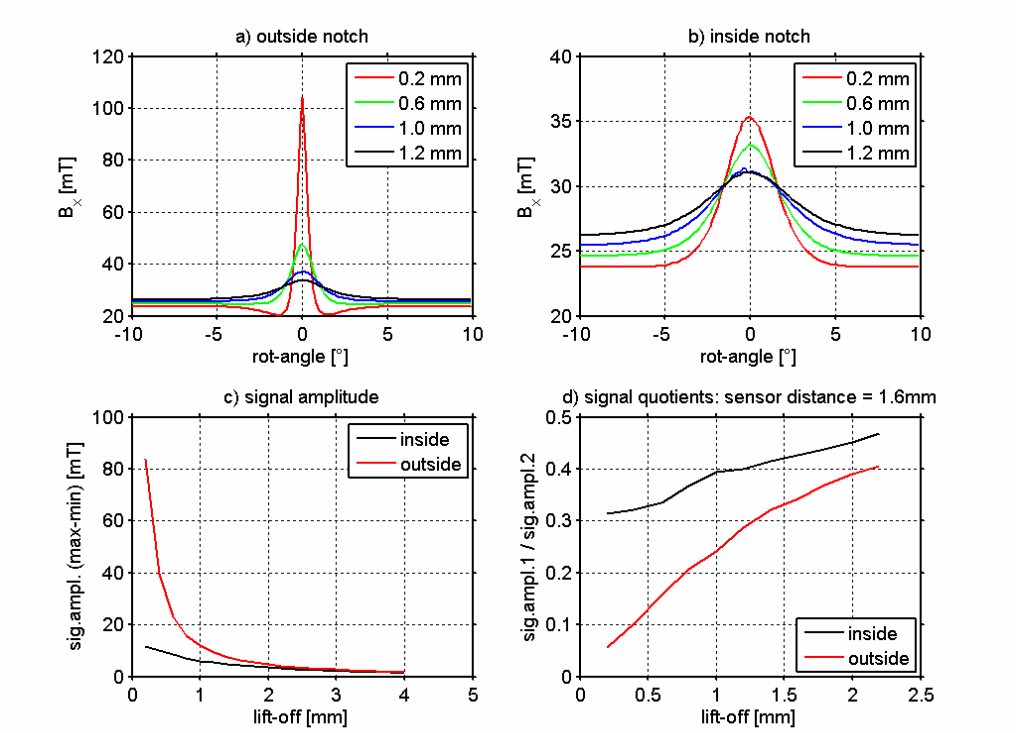

Figure 7: lift-off effect for inside and outside notches: all above figures were results from a 72x4mm pipe, a 0.2x0.5 mm (width x depth) notch and a magnetizing current of 2 A. Subfigures a) and b) show the simulated signals for outside notch and inside notch, respectively, for different lift-off heights as indicated in the figures legend. Subfigure c) displays the signal-amplitudes (i.e. maximum B_x – minimum B_x) as a function of the lift-off. In d) the relation of the signal amplitudes for two sensors, one at the indicated lift-off and the second at 1.6mm above, are displayed.

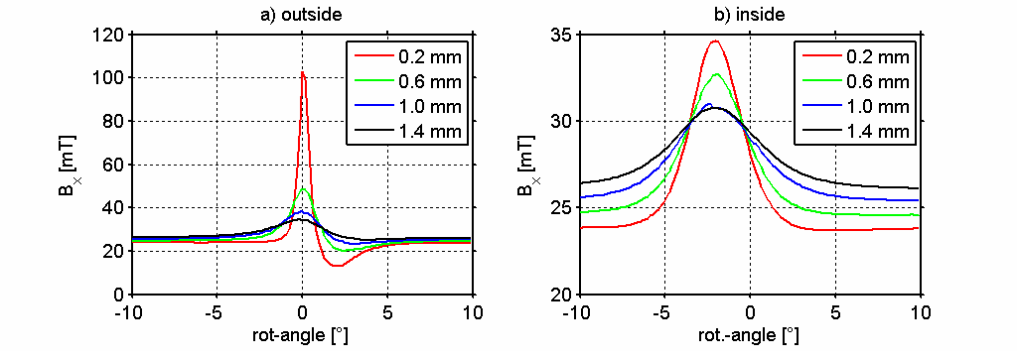

Figure 8: comparison of an inside and outside tilted notch: the notch size is 0.1 x 1.5 mm (width x depth) large and tilted at an angle of 60°. Subfigure a) and b) show MFL signals for the outside and inside case respectively for different values of lift-off.

As a last example we present in **Figure 8** the results of a calculation comparing inside and outside tilted notches. As opposed to the outside notch no asymmetry can be detected from the calculated signal for an inside notch. Instead, the peak in the signal is shifted towards a rotation angle in the near of the endpoint of the tilted notch. Practically it seems impossible to separate oblique from perpendicular notches in the inside case. The inside oblique notch is looking like a broader defect from the outside. The lift-off dependence of the outside oblique notch is basically the same as for the perpendicular case, compare **Figure 3**.

3. Summary and Conclusions

From the above discussion of the first results of our FEM calculations of MFL signals some main conclusions can be drawn:

- There is a linear increase of signal amplitude with notch depth for outside case.
- In the inside situation there exists an even stronger (perhaps quadratic) increase with notch depth.
- The signal decreases exponentially with increasing lift-off.
- Increasing the notch-width of an outside notch first increases the signal amplitude, than a maximum is reached (depending on lift-off) and for even broader notches the signal decreases. The signal FWHM increases with notch width almost linearly (for outside notch).
- Tilted notches lead to asymmetric signals for outside defect, and to a shift in signal position for inside defects.
- The measurements discussed in [13] concerning the separation of outside and inside defects are confirmed.

All the calculations presented here were performed for only one specific pipe geometry and material, but can easily be repeated for different situations. Some main goals for further activities based on the presented work are:

- Model further defects, like larger or smaller defects or different (non-rectangular) shape, simulate the effect of wall thickness modulation and non-uniform material parameters.
- Implement strategies for type of defect separation (at least inside / outside separation) based on the above results.
- Use results based on calculations of signal amplitude as a function of pipe geometry to reduce the number of necessary test-pipes for mill installations.

References

[1] C. Mandache, L. Clapham, *J.Phys. D: Appl. Phys.* **36**, 2427 (2003)
[2] C. Edwards, S.B. Palmer, *J.Phys. D: Appl. Phys.* **19**, 657 (1986)
[3] W. Lord, *IEEE Trans. Mag.* **MAG-19**, 2437 (1983), and references therein
[4] B. Brudar, *NDT Int.* **18**, 353 (1985)
[5] F. Förster, *NDT Int.* **19**, 3 (1986)
[6] D.L. Atherton, M.G. Daly, *NDT Int.* **20**, 235 (1987)
[7] http://www.wfndec.org/benchmarkproblems.htm
[8] J. Etcheverry, A. Pignotti, G. Sanchez, P. Stickar, *Rev. Quant. NDE* **22,** 1824 (2003), and references therein
[9] V. Lunin, D. Alexeevsky, *Rev. Quant. NDE* **22**, 1830 (2003)
[10] Z. Zeng, Y. Tian, S. Upda, L. Upda, *Rev. Quant. NDE* **23**, 1553 (2004)
[11] M. Ruch, J.P. A. Bastos, *Insight* **46,** 736 (2004)
[12] H. Zuoying, Q. Peiwen, C. Liang, *NDT&E Int.* **39**, 61 (2005)
[13] Th. Orth, M. Kaack, S. Nitsche, Ch. Delhaes, *DGZfP-Berichtsband* **94**, P40 (2005)
[15] www.comsol.com
[16] www.mathworks.com